doi:10.1093/brain/awr361 Brain 2012: 135; 736–750 | 736

BRAIN
A JOURNAL OF NEUROLOGY

Frontotemporal dementia with the *C9ORF72* hexanucleotide repeat expansion: clinical, neuroanatomical and neuropathological features

Colin J. Mahoney,[1,*] Jon Beck,[2,*] Jonathan D. Rohrer,[1] Tammaryn Lashley,[3] Kin Mok,[4] Tim Shakespeare,[1] Tom Yeatman,[1] Elizabeth K. Warrington,[1] Jonathan M. Schott,[1] Nick C. Fox,[1] Martin N. Rossor,[1] John Hardy,[4] John Collinge,[3] Tamas Revesz,[3] Simon Mead[2,*] and Jason D. Warren[1,*]

1 Dementia Research Centre, Department of Neurodegenerative Diseases, UCL Institute of Neurology, London WC1N 3BG, UK
2 MRC Prion Unit, Department of Neurodegenerative Diseases, UCL Institute of Neurology, London WC1N 3BG, UK
3 Queen Square Brain Bank, Department of Molecular Neuroscience, UCL Institute of Neurology, London WC1N 3BG, UK
4 Reta Lila Weston Research Laboratories, Departments of Molecular Neuroscience and of Clinical Neuroscience, UCL Institute of Neurology, London WC1N 3BG, UK

*These authors contributed equally to this work.

Correspondence to: Dr Jason D. Warren,
Dementia Research Centre,
UCL Institute of Neurology,
London WC1N 3BG, UK
E-mail: jwarren@drc.ion.ucl.ac.uk

An expanded hexanucleotide repeat in the *C9ORF72* gene has recently been identified as a major cause of familial frontotemporal lobar degeneration and motor neuron disease, including cases previously identified as linked to chromosome 9. Here we present a detailed retrospective clinical, neuroimaging and histopathological analysis of a *C9ORF72* mutation case series in relation to other forms of genetically determined frontotemporal lobar degeneration ascertained at a specialist centre. Eighteen probands (19 cases in total) were identified, representing 35% of frontotemporal lobar degeneration cases with identified mutations, 36% of cases with clinical evidence of motor neuron disease and 7% of the entire cohort. Thirty-three per cent of these *C9ORF72* cases had no identified relevant family history. Families showed wide variation in clinical onset (43–68 years) and duration (1.7–22 years). The most common presenting syndrome (comprising a half of cases) was behavioural variant frontotemporal dementia, however, there was substantial clinical heterogeneity across the *C9ORF72* mutation cohort. Sixty per cent of cases developed clinical features consistent with motor neuron disease during the period of follow-up. Anxiety and agitation and memory impairment were prominent features (between a half to two-thirds of cases), and dominant parietal dysfunction was also frequent. Affected individuals showed variable magnetic resonance imaging findings; however, relative to healthy controls, the group as a whole showed extensive thinning of frontal, temporal and parietal cortices, subcortical grey matter atrophy including thalamus and cerebellum and involvement of long intrahemispheric, commissural and corticospinal tracts. The neuroimaging profile of the *C9ORF72* expansion was significantly more symmetrical than progranulin mutations with significantly less temporal lobe involvement than microtubule-associated protein tau mutations. Neuropathological examination in six cases with *C9ORF72* mutation from the frontotemporal lobar degeneration series identified histomorphological features

Received November 23, 2011. Revised December 16, 2011. Accepted December 19, 2011

consistent with either type A or B TAR DNA-binding protein-43 deposition; however, p62-positive (in excess of TAR DNA-binding protein-43 positive) neuronal cytoplasmic inclusions in hippocampus and cerebellum were a consistent feature of these cases, in contrast to the similar frequency of p62 and TAR DNA-binding protein-43 deposition in 53 control cases with frontotemporal lobar degeneration–TAR DNA-binding protein. These findings corroborate the clinical importance of the *C9ORF72* mutation in frontotemporal lobar degeneration, delineate phenotypic and neuropathological features that could help to guide genetic testing, and suggest hypotheses for elucidating the neurobiology of a culprit subcortical network.

Keywords: frontotemporal lobar degeneration; motor neuron disease; neurodegenerative disorders; neuroimaging; genetics

Abbreviations: FTD = frontotemporal dementia; FTLD = frontotemporal lobar degeneration; MND = motor neuron disease; TDP = TAR DNA-binding protein

Introduction

The frontotemporal lobar degenerations (FTLD) are a common cause of young onset neurodegeneration (Ratnavalli *et al.*, 2002). FTLD is clinically and pathologically heterogeneous (Lillo *et al.*, 2010; Seelaar *et al.*, 2011) and genetic factors play a significant role, with a genetic basis implicated in up to 40% of cases in series from specialist centres (Rohrer *et al.*, 2009; Rohrer and Warren, 2011). Discovery of disease-causing mutations in the progranulin (*GRN*) and microtubulin-associated protein tau *(MAPT)* genes left a substantial minority of cases of autosomal dominant FTLD without an identified genetic substrate; however, linkage to chromosome 9p21 has been described in a number of families with phenotypes of frontotemporal dementia (FTD), motor neuron disease (MND) or overlap syndrome (Morita *et al.*, 2006; Vance *et al.*, 2006; Valdmanis *et al.*, 2007; Luty *et al.*, 2008; Le Ber *et al.*, 2009; Gijselinck *et al.*, 2010; Boxer *et al.*, 2011; Pearson *et al.*, 2011). This elusive chromosome 9 gene has recently been identified as an expanded hexanucleotide (GGGGCC) repeat insertion in a non-coding promoter region of open reading frame 72 (*C9ORF72)* and is likely to account for a substantial proportion of the remaining genetic susceptibility to FTLD and MND) (Dejesus-Hernandez *et al.*, 2011; Gijselinck *et al.*, 2011; Renton *et al.*, 2011). Cases with the *C9ORF72* repeat expansion with histopathological correlation have had TAR DNA-binding protein (TDP)-43 deposition, however, the pathogenic mechanism whereby the expansion leads to neurodegeneration has not been defined.

As has been demonstrated previously in the case of *MAPT* and *GRN*-associated FTLD (Rademakers *et al.*, 2007; Beck *et al.*, 2008; Le Ber *et al.*, 2008; Rohrer and Warren, 2011) detailed phenotypic characterization of disease-causing mutations has both clinical and neurobiological implications. Clinically, such a characterization will help guide genetic screening and thereby facilitate early, accurate diagnosis, and ultimately the possibility of identifying individuals both with established and incipient disease for clinical trials of disease-modifying therapies. Neurobiologically, phenotypic information may help elucidate the pathophysiology of the disease, for example, by delineating the interaction of the molecular lesion with affected neural networks (Fletcher and Warren, 2011; Rohrer *et al.*, 2011). Here we describe the clinical, neuropsychological, neuroimaging and neuropathological features of a large series of cases with the *C9ORF72* hexanucleotide repeat expansion ascertained at a tertiary referral centre.

Subjects and methods

Case ascertainment

The University College London FTLD DNA cohort comprises 273 cases (256 probands) with a syndromic diagnosis within the FTLD spectrum (Litvan *et al.*, 1996; Boeve *et al.*, 2003; Gorno-Tempini *et al.*, 2011; Rascovsky *et al.*, 2011), including 122 patients with behavioural variant FTD, 11 patients with FTD and MND (FTD–MND), 53 patients with semantic dementia, 49 patients with progressive non-fluent aphasia, 18 patients with corticobasal syndrome, eight patients with a progressive non-fluent aphasia–corticobasal overlap syndrome, 11 patients with progressive supranuclear palsy syndrome and one patient with the inclusion body myopathy–Paget's disease–frontal dementia syndrome. DNA is also held on a further 11 patients with the logopenic aphasia variant of primary progressive aphasia (Gorno-Tempini *et al.*, 2011). The cohort includes 22 cases with *MAPT* mutations (15 probands), 24 cases with *GRN* mutations (17 probands) and one case with a valosin-containing protein (*VCP)* mutation (Table 1). Thus, 223 probands with FTLD syndromes and 11 individuals with logopenic aphasia lacking a previously identified pathogenic mutation were included in the present screen for the *C9ORF72* repeat expansion. Prior to screening, all cases within the cohort were assigned a modified Goldman score as a measure of the extent of family history of the disease (Goldman *et al.*, 2005; Beck *et al.*, 2008; Rohrer *et al.*, 2009). A score of 1 represents an autosomal dominant family history of FTLD or MND; 2 is familial aggregation of three or more family members with dementia; 3 is one other first-degree relative with dementia of young onset (<65 years); 3.5 is one other first-degree relative with dementia of onset >65 years of age; and 4 is no or unknown family history. Of the probands with a diagnosis within the FTLD spectrum included in the screen, six had a Goldman score of 1; 26 had a score of 2; 12 had a score of 3; 22 had a score of 3.5; and 157 had a score of 4 (Table 1).

Ethical approval for the study was obtained from the local institutional ethics committee and carried out in accordance with the Declaration of Helsinki.

Table 1 Numerical data on mutation frequency, demographics and family history for cases in this series

					n (% total) per modified Goldman score				
Group	*n*	Male (%)	AAO (SD)	Probands (% totals)	1 (%)	2 (%)	3 (%)	3.5 (%)	4 (%)
C9ORF72	19	58	55.1 (6.6)	18 (7.0)	4 (23.5)	6 (17.6)	1 (5.6)	1 (4.2)	6 (3.7)
MAPT	22	59	51.7 (6.9)	15 (5.9)	6 (35.3)	3 (8.8)	3 (16.7)	1 (4.2)	2 (1.2)
GRN	24	50	57.6 (6.5)	17 (6.6)	4 (23.5)	5 (14.7)	3 (16.7)	1 (4.2)	4 (2.5)
VCP	1	100	44.0	1 (0.4)	1 (5.9)	0	0	0	0
Others	207	57	59.0 (8.6)	205 (80.1)	2 (11.8)	20 (58.8)	11 (61.1)	21 (87.5)	151 (92.6)
Total	273			256	17	34	18	24	163

In summary, if the modified Goldman score is 1, 88% of patients have a known genetic abnormality, and this percentage decreases with a higher score: 41% if the score is 2, 39% if the score is 3, 13% if the score is 3.5 and 7% if the score is 4. AAO = age at onset.

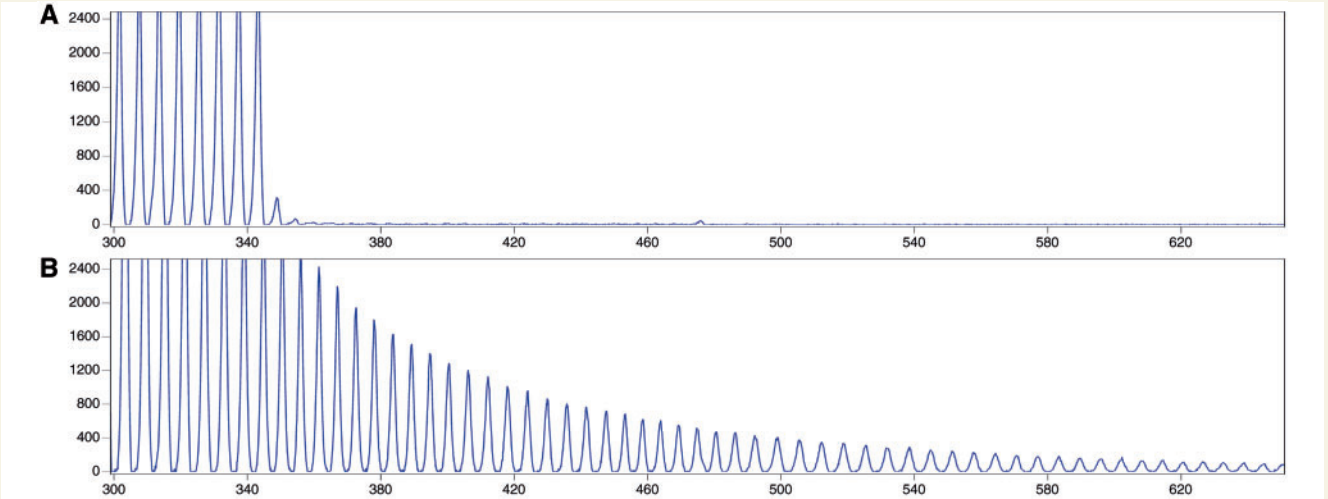

Figure 1 Examples of electrophoresed products of repeat-primed polymerase chain reaction used to detect expansions in *C9ORF72*. Each panel was scaled to 800 fluorescent units on the *y*-axis and between 300–650 bp on the *x*-axis. (**A**) Data from a FTLD patient sample without an expansion and (**B**) data from a patient with FTLD with 2 and >60 repeats.

Genetic analyses

All samples with genetically unexplained FTLD based on previous screens were assessed for *C9ORF72* expansions using the repeat-primed polymerase chain reaction as previously published (Renton *et al.*, 2011). Mutations were called if repeats of this assay consistently showed more than 30 repeats in total (Fig. 1).

Clinical and neuropsychological analyses

A retrospective review of clinical case notes and neuropsychological reports (where available) was undertaken in those cases identified as having the *C9ORF72* repeat expansion. Demographic features, family history and disease duration were recorded. Earliest clinical features were extracted by an experienced neurologist, and neuropsychological features at first assessment were also recorded; 13 participants had undergone more than one clinical assessment, and clinical features at the final assessment were also recorded. Demographic data for *C9ORF72* cases were compared statistically with *MAPT* and *GRN* mutation groups using two-tailed *t*-tests within STATA 10 (Statacorp).

In addition, we recorded results of laboratory investigations undertaken as part of the clinical evaluation of *C9ORF72* cases: electrophysiological assessments and CSF examination [including $A\beta_{1-42}$ level (*Innotest* β-amyloid$_{1-42,}$ Innogenetics), total tau (*Innotest* hTau Ag, Innogenetics) and S100 beta (Abnova)].

Neuroimaging analyses

A majority of patients included in the University College London FTLD cohort have had at least one T_1-weighted magnetic resonance brain volume acquired on either a 1.5T GE Signa scanner (General Electric) (256 × 256 matrix; 1.5 cm slice thickness) or a 3.0T Siemens Trio scanner (Siemens) (256 × 256 matrix; 1.1 cm slice thickness). Where available, volumetric brain MRI data for the *C9ORF72* mutation cases were analysed using previously described semi-automated techniques and compared with the *GRN* and *MAPT* mutation groups.

Whole-brain segmentation yielded a whole-brain region separated from CSF, dura and skull (Freeborough *et al.*, 1997). Scans were then transformed into standard space by registration to the Montreal Neurological Institute template and hemispheric volumes were calculated for each individual. In order to assess hemispheric asymmetry, a left/right asymmetry ratio was derived in each case by dividing the left hemispheric volume by the right hemispheric volume, as previously described (Rohrer *et al.*, 2010). Repeat scans were transformed into standard space and underwent an affine registration (12 degrees of freedom) onto the baseline scan. Volume change was calculated directly from registered scans using the brain boundary shift integral (Freeborough and Fox, 1997). Brain boundary shift integral-derived whole-brain volume changes were expressed as an annualized volume change in ml per year. Volumetric data from a previously published cohort (Rohrer *et al.*, 2010) of *GRN* [$n = 4$, mean interval 1.3 years, standard deviation (SD) 0.2] and *MAPT* ($n = 6$, 2.1 years, SD 1.0) mutation carriers (all values derived using the same methods) were compared against *C9ORF72* mutation carriers using two-sample *t*-tests with unequal variance within STATA 10 (Statacorp).

In order to determine patterns of brain atrophy at group level, volumetric MRI data from healthy controls and the *C9ORF72*, *MAPT* and *GRN* mutation groups were compared using voxel-based morphometry with the DARTEL toolbox of SPM8 (http://www.fil.ion.ucl.ac.uk/spm) running under Matlab 7.0 (Mathworks). Segmentation, modulation and smoothing of grey and white matter images were performed using default parameter settings. Final images were normalized to standard space. In order to reduce the effects of atrophy, analysis was performed over voxels within a consensus mask, which includes all voxels with intensity of >0.1 in 70% of subjects (Ridgway *et al.*, 2009). A multiple regression analysis was performed with voxel intensity modelled as a function of group membership with age, total intracranial volume, gender and scanner field strength included as nuisance covariates. Results were then overlaid on the MNI152 template brain for anatomical analysis. Total intracranial volume was calculated by summing together grey matter, white matter and CSF segmentations.

Cortical thickness measurements were made using FreeSurfer v5.1 (http://surfer.nmr.mgh.harvard.edu/) following previously described methods (Dale *et al.*, 1999; Fischl and Dale, 2000). A surface-based Gaussian smoothing kernel of 20 mm full width at half-maximum was applied to reduce local variations in cortical thickness. Skull stripping used a locally generated brain mask, and FreeSurfer ventricular segmentations were added to the white matter mask to improve cortical segmentation. Between-group variations in cortical thickness were assessed using a vertex-by-vertex general linear model performed with SurfStat (http://www.math.mcgill.ca/keith/surfstat/). Regional differences in grey matter between control and disease groups were assessed using the same covariates as the voxel-based morphometry analysis. A significance threshold of $P < 0.05$ with false discovery rate correction was applied. Where this threshold was not met, percentage difference maps were used to illustrate trends in atrophy patterns.

Alterations of white matter tract integrity were assessed with diffusion tensor imaging using an unbiased group-wise analysis technique. Three individuals underwent diffusion tensor imaging scanning on the same 3T scanner (64 direction single shot, spin-echo-echo planar imaging sequence, 55 contiguous slices). Tensor eigenvalues ($\lambda1$ = axial diffusivity, $\lambda2$ and $\lambda3$), fractional anisotropy and radial diffusivity (RD = $\lambda2 + \lambda3$) were extracted at each voxel using CAMINO (Cook *et al.*, 2006). Tensor fitted images were then imported for voxel-wise analysis within tract-based spatial statistic (TBSS v1.1) (Smith *et al.*, 2006). Voxel intensity within tracts was modelled on disease group membership with the age, gender and total intracranial volume included as nuisance covariates. Statistical analysis was implemented using the permutation-based (non-parametric) randomize tool within FSL.

For all group-wise analyses, a significance threshold ($P < 0.05$) was applied following correction for multiple comparisons. Threshold-free cluster enhancement modulation was applied to diffusion tensor imaging results (Smith and Nichols, 2009).

Neuropathological protocol

Cases in the University College London FTLD cohort coming to post-mortem have undergone detailed histopathological assessment as previously described (Lashley *et al.*, 2011; Rohrer *et al.*, 2011). At the time of brain donation, brains were fixed in 10% buffered formaldehyde and sampled using standard protocols. Histological sections of hippocampus with parahippocampal and fusiform gyri and cerebellum, stained with antibodies to p62 (1:200, BD Transduction Laboratories) and TDP-43 (amino acids 1-261, Abnova, 1:800), were analysed. Selection of these anatomical regions was based on preliminary observations indicating that the number of p62-positive inclusions may exceed TDP-43-positive neuronal cytoplasmic inclusions in *C9ORF72* mutation cases; using a semi-quantitative approach, the frequency of p62-positive neuronal cytoplasmic inclusions was compared with TDP-43-positive inclusions in the granule cell layer of the dentate fascia, hippocampal subregions and cerebellar granule cell layer.

Results

Genetics

Of the 223 cases with FTLD screened, 18 probands (8% of probands without previously identified mutations) were found to have the *C9ORF72* repeat expansion. One further case in the cohort, from the same family as one of the probands, also had the *C9ORF72* expansion. No mutations were identified in the 11 screened cases with logopenic aphasia. Alternatively expressed, 18/51 (35%) of all FTLD probands with identified mutations or 18/256 (7%) of all probands in our FTLD series had a *C9ORF72* mutation. Of the 18 *C9ORF72* probands, four patients had a modified Goldman score of 1, six had a score of 2, one had a score of 3, one had a score of 3.5 and six had a score of 4 (Fig. 2 and Table 1), indicating that in this series 6/163 (4%) of apparently sporadic cases of FTLD had a *C9ORF72* mutation. If an individual had a Goldman score of 1 assigned, a genetic cause

(*C9ORF72*, *MAPT*, *GRN* or *VCP* mutation) was identified in 88% of all FTLD probands, of which 35% were *MAPT*, 24% were *C9ORF72*, 24% were *GRN* and 6% were *VCP* mutations. If a score of 2 was assigned, a genetic cause was identified in 41% of cases; if a score of 3 was assigned, a genetic cause was identified in 39%; if a score of 3.5 was identified, a genetic cause was identified in 13% and if a score of 4 was assigned, a genetic cause was identified in 7% of cases. Representative pedigrees of *C9ORF72* families are shown in Fig. 3. The pedigree data indicate that age at symptom onset and clinical syndrome are highly variable within a family.

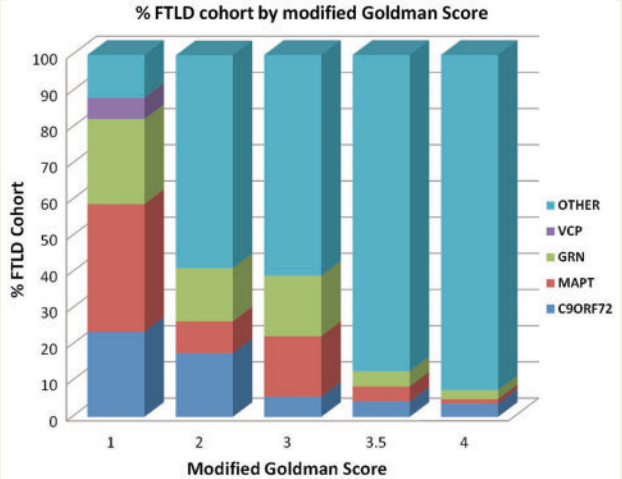

Figure 2 FTLD DNA cohort by modified Goldman score. Each bar displays % of cohort by assigned Goldman score and mutation status.

Clinical and neuropsychological features

The average age at onset across the series was 55.0 years (SD 6.6, range 43–68), which did not differ significantly from *MAPT* or *GRN* mutation groups. Mean disease duration from symptom onset until death ($n = 12$) or time of last review (still alive $n = 5$) was 8.7 years (SD 4.9, range 1.7–22), which was not significantly different to either the *MAPT* mutation group (11.4 SD 5.3 years) or the *GRN* mutation group (6.8 SD 2.3 years). As a proportion of the entire FTLD cohort, 11% of cases with behavioural variant FTD, 36% with FTD–MND and 2% with progressive non-fluent aphasia were found to have the *C9ORF72* repeat expansion.

Detailed clinical information was available on 16 of the 19 cases with the *C9ORF72* expansion who had been assessed in the specialist cognitive disorders clinic at the National Hospital for Neurology and Neurosurgery. Fifteen patients had neuropsychological assessments. Group data for these cases are summarized in Fig. 4 and individual data in Table 2. The mean duration of follow-up was 2.3 (SD 1.4) years. At initial presentation, eight of these 16 patients (50% of cases) had a clinical syndromic diagnosis of behavioural variant FTD; three (19%) had a diagnosis of FTD–MND; two (13%) had a diagnosis of probable Alzheimer's disease; one had a diagnosis of progressive non-fluent aphasia, one an encephalitic illness and one atypical Parkinsonism. The final syndromic diagnoses were behavioural variant FTD in 12 cases, FTD–MND in three cases and progressive non-fluent

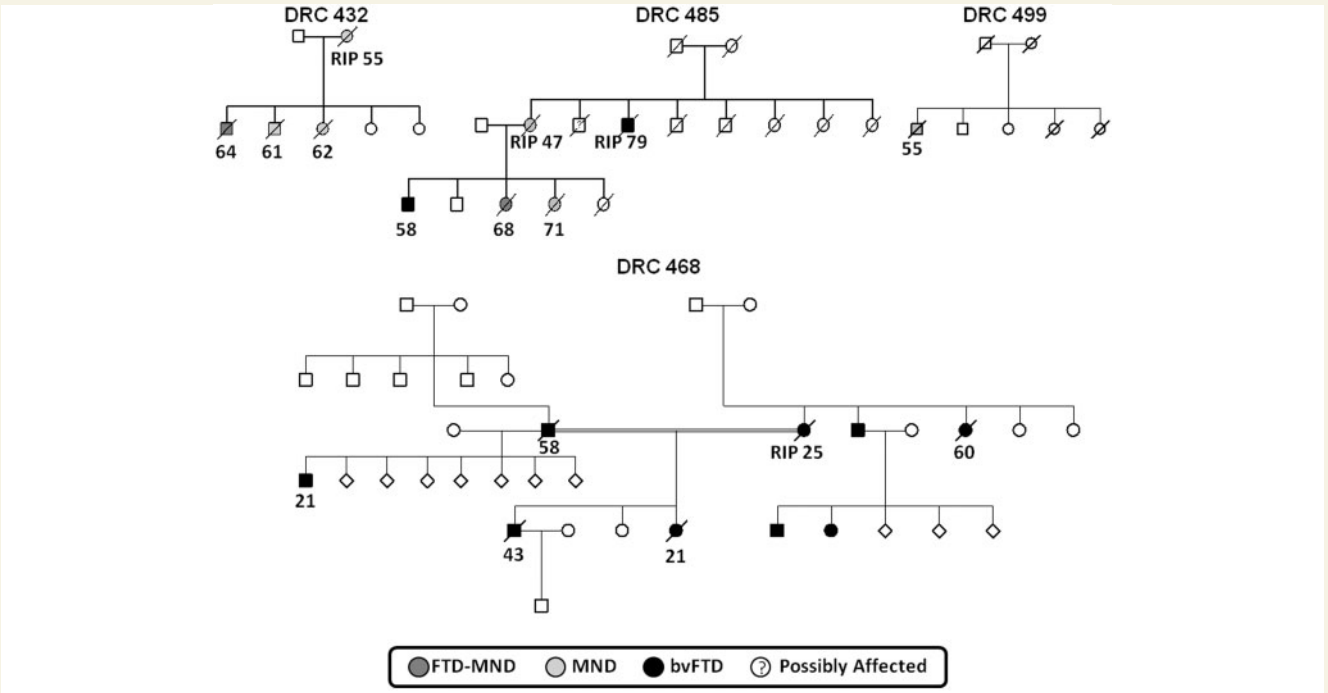

Figure 3 Representative pedigrees from the Dementia Research Centre (DRC) cohort indicating inheritance, predominant clinical syndrome and, where known, age at onset (RIP indicates only age at death known). bvFTD = behavioural variant FTD.

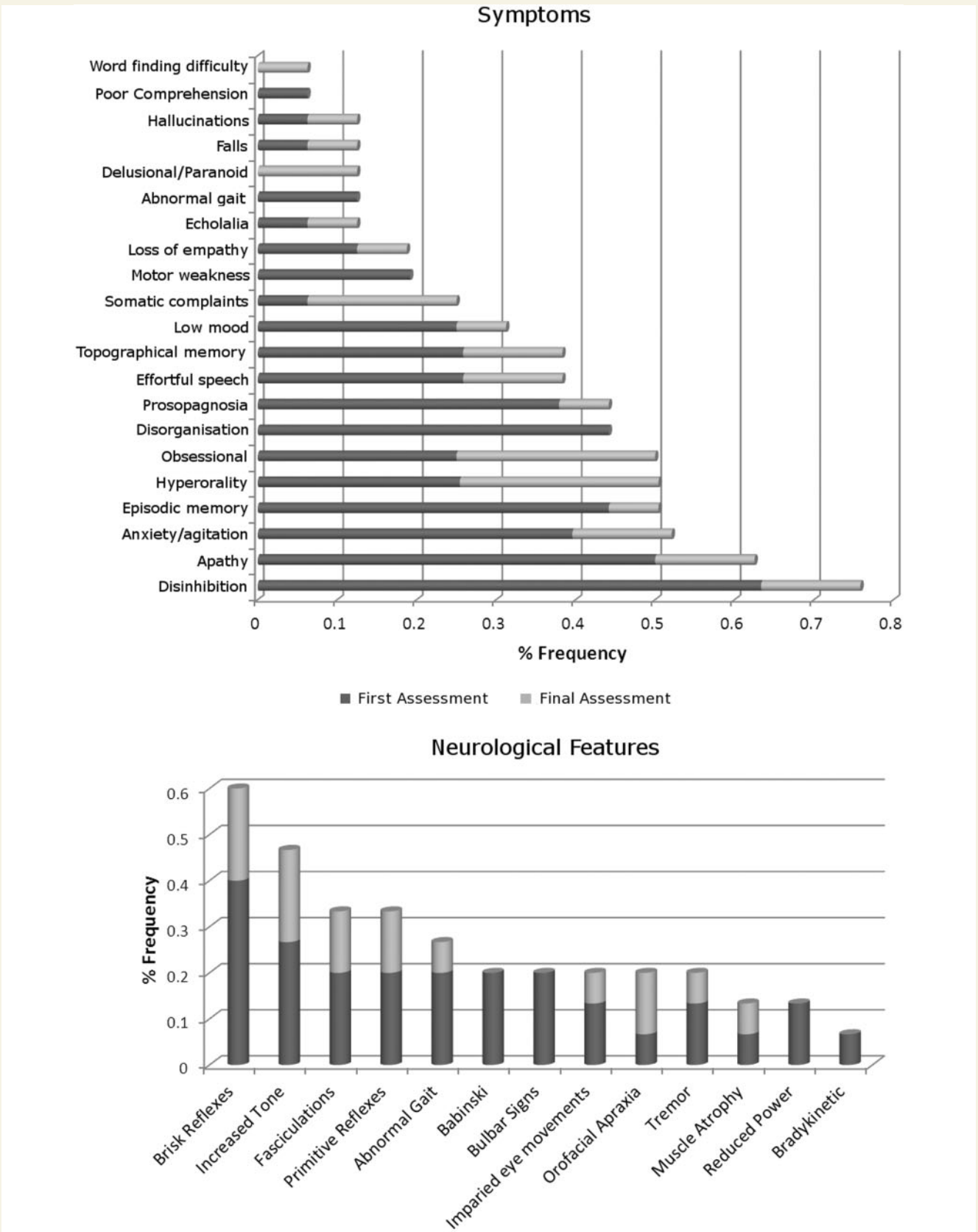

Figure 4 Prevalence of symptoms and neurological signs (expressed as proportion of disease cohort) observed in *C9ORF72* cases. Data for first and final assessments are coded separately.

Table 2 Individual clinical and neuropsychological data available for *C9ORF72* cases

Case	Final diagnosis	AAO (years)	Duration (years)	Hand	Early symptoms	Neuropsychology profile								
						VIQ	PIQ	RMTW[a]	RMTF[a]	GNT[a]	Calc[a]	Percep[a]	Exec	Praxis
1	bvFTD	51	6.0	R	Anxiety, disinhibition, episodic memory impairment, speech adynamic	80	89	<5	<1	50–75	<1	>5	+ +	Norm
2	bvFTD	60	7.0[b]	R	Anxiety, delusions, disinhibition, episodic memory impairment, hyperorality	100	113	5–10	<5	95	<50	>5	+ +	Norm
3	bvFTD	56	8.0[b]		Anxiety, empathy loss, obsessionality, prosopagnosia	82	77	<5	10–25	<5	5–10	>5	+ +	Imp
4	FTD–MND	55	7.7		Disinhibition, obsessionality, speech effortful, weakness upper limbs									Norm
5	bvFTD	45	8.4	L	Anxiety, apathy, depression, involuntary movements	71	75	<5		<5	<5	>5	+ +	
6	bvFTD	55	7.1		Disorganization, episodic memory impairment, obsessionality	87	78	<5	<1	<5	5–10	>5	+ +	Imp
7	bvFTD	55	16.6		Disorganization, empathy loss, episodic memory impairment, prosopagnosia	103	95	50–75	<1	75	25–50	>5	+ +	
8	bvFTD	43	1.7	R	Anxiety, apathy, disinhibition, prosopagnosia, topographical memory impairment	UT	UT	UT	UT	5	<5	>5	+	Imp
9	FTD–MND	64	5.4	R	Apathy, delusions, prosopagnosia, speech effortful, topographical memory impairment	84	82	5–10	<1	<5	<5	>5	+ +	Norm
10	FTD–MND	54	5.0	R	Depression, disinhibition, speech effortful, weakness limbs	69	80	5–10	1–5	10–25	<5	>5	+	Imp
11	bvFTD	58	8.0[b]	R	Apathy, disinhibition, hyperorality, topographical memory impairment	85	69	10–25	50–75	10–25	<50	>5	+ + +	Imp
12	bvFTD	61	5.7	R	Episodic memory impairment, hyperorality, falls, somatic symptoms, weakness limbs	78	76	<1	<1	<5	10–25	>5	+ + +	Imp
13	bvFTD	68	7.1	R	Apathy, episodic and topographical memory impairment, speech adynamic	73	78	<5	<5	10–25	10–25	>5	+ +	Imp
14	bvFTD	53	14.8		Apathy, disinhibition, episodic memory impairment, prosopagnosia	UT	UT	<5	<5	<1	UT	>5	+	Imp
15	PNFA	55	5.0[b]	R	Comprehension impairment, disinhibition, speech effortful	55	70	25–50	<1	<5	<1	>5	+ + +	Norm
16	bvFTD	46	22.0[b]	R	Anxiety, disorganization, episodic memory impairment, obsessionality, prosopagnosia	116	113	75–95	50–75	75–90	>90	>5	+ +	Norm

Blank cells indicate testing not performed.
a Percentile scores are shown.
b Current duration for living cases.
+/+ +/+ + + = defective performance on at least one/two/three tests, respectively, of executive function (Weigl sorting test; Wisconsin Card Sorting Test; Stroop colour interference; Verbal Fluency).
AAO = age at onset; bvFTD = behavioural variant FTD; Calc = calculation; Dur = total/current disease duration; Exec = executive functions; GNT = Graded Naming Test; Hand = handedness data available; Imp = impaired; Norm = normal; Percep = perception; PIQ = performance IQ; PNFA = progressive non-fluent aphasia; RMTF/W = recognition memory test for faces/words; UT = untestable; VIQ = verbal IQ.

aphasia in one case. For the remaining three cases without detailed clinical information, the final diagnoses were behavioural variant FTD in two cases and FTD–MND in one case.

The most common symptoms at the time of first presentation (Fig. 4) were disinhibition (63%) and apathy (49%); however, forgetfulness (44%) and anxiety (38%) were also prominent. Based on the history obtained from patients' carers, the most common initial symptom was anxiety (33%), followed by disinhibition (13%), effortful speech (13%) and impaired topographical memory (13%). At the time of final assessment, the most frequent symptoms were disinhibition (76%), apathy/adynamia (63%), and anxiety (52%). The most common neuropsychological features (Table 2) were executive dysfunction (100%), impaired verbal and/or visual episodic memory (87%), apraxia (57%), anomia (47%) and dyscalculia (38%). Object and space perception were unimpaired in all patients assessed. The most common physical neurological sign at presentation was brisk deep tendon reflexes (40%); fewer than 20% of patients had features of bulbar or lower motor neuron involvement. At the time of final assessment (or first if only one assessment), the most frequent neurological signs were brisk tendon reflexes (60%), spasticity (47%), fasciculations (33%) and primitive reflexes (33%).

Four patients (two with an initial clinical diagnosis of FTD–MND) underwent electrophysiological studies; one individual had EMG evidence of MND, one had borderline features and two had no features of MND. Five patients underwent CSF examination. Basic CSF constituents including protein, cells and glucose were within normal limits for all patients examined; further analyses comprised $A\beta_{1-42}$ (mean = 465 pg/ml, SD 303, in-house normal range = 220–2000; all within the normal range), total tau (mean = 190 pg/ml, SD 103, in-house normal range = 0–32; 80% of cases within the normal range) and S100 beta (mean = 0.33 ng/ml, SD 0.1, in-house normal range = 0.05–0.61; all within the normal range). The mean tau-to-beta-amyloid ratio was 0.5 (SD 0.3) and also within the normal limits for the assaying laboratory for all subjects.

Neuroimaging features

Volumetric data

Eleven patients with the *C9ORF72* repeat expansion (mean age 58.5, SD 8.3 years) underwent volumetric brain MRI: eight at 1.5T and three at 3.0T. Five patients had repeat volumetric MRI on the same scanner (mean interval 1.2 years, SD 0.6), four at 1.5T and one at 3T. Inspection of individual brain magnetic resonance scans revealed highly variable profiles of frontal, temporal and parietal lobe atrophy; representative sections are shown in Fig. 5.

For the purposes of the group-wise analysis, neuroimaging data from the *C9ORF72* mutation group were compared with a group of 15 age- and gender-matched healthy control subjects (mean age 58.6, SD 5.7 years); brain images were acquired for 12 controls on the same 1.5T magnetic resonance scanner and for three controls on the same 3T scanner as the patients, and all group-wise analyses were adjusted for variation in field strength. Mean brain volume corrected for total intracranial volume was significantly lower in the *C9ORF72* mutation group (Fig. 6) (mean brain/total intracranial volume ratio = 0.68, SD 0.07; $P = 0.001$) than the control group (mean brain/total intracranial volume = 0.77, SD 0.03); mean brain volume did not differ significantly between the *C9ORF72* mutation group and the *MAPT* or *PGRN* mutation groups. Mean annualized atrophy rate was greatest in the *GRN* mutation group (Fig. 6) (brain boundary shift integral change 3.4%/year, SD 0.6) followed by the *C9ORF72* mutation group (brain boundary shift integral change 1.6%/year, SD 1.6) and the *MAPT* mutation group (brain boundary shift integral change 1.4%, SD 0.6), but mean atrophy rates did not differ significantly between groups. As indexed using the hemispheric asymmetry ratio, cerebral atrophy was relatively symmetric in the *C9ORF72* mutation group (Fig. 6) (hemispheric asymmetry ratio range 0.96–1.04) and the *MAPT* mutation group (range 0.97–1.05), similar to the healthy control group (range 0.98–1.02); whereas cerebral atrophy was strongly asymmetric in the *GRN* mutation group (range 0.86–1.33).

Unbiased analyses

In the voxel-based morphometry analysis, relative to the healthy control group ($n = 15$), the *C9ORF72* mutation group ($n = 11$) showed a regional profile of grey matter atrophy including thalamus bilaterally, left opercular cortex, left orbitofrontal cortex and bilateral posterior cerebellum (all false discovery rate corrected $P < 0.05$; Fig. 7). Direct comparisons between the *C9ORF72* mutation group and the *MAPT* mutation group ($n = 11$) (Fig. 8) showed the *MAPT* group had decreased grey matter bilaterally in anterior temporal lobe, amygdala, hippocampus and parahippocampal gyrus (all false discovery rate corrected $P < 0.05$), while the *C9ORF72* group had decreased grey matter in prefrontal cortex and cerebellar vermis (uncorrected $P < 0.001$). Direct comparisons between the *C9ORF72* mutation group and the *GRN* mutation group ($n = 8$) (Fig. 8) showed that the *GRN* group had decreased grey matter asymmetrically in left inferior and middle temporal gyri, post-central gyrus and inferior frontal gyrus, whereas the *C9ORF72* group had decreased grey matter in right prefrontal cortex (all uncorrected $P < 0.001$).

In the cortical thickness analyses, relative to healthy controls, the *C9ORF72* mutation group showed a symmetrical pattern of reduced thickness of frontal, anterior and superior temporal and parietal cortices (Fig. 7). Direct comparisons between the *C9ORF72* and *MAPT* mutation groups showed the *MAPT* group had reduced thickness of anterior temporal cortex bilaterally (false discovery rate corrected $P < 0.05$) (Fig. 8). Direct comparisons between the *C9ORF72* and *GRN* mutation groups showed the *GRN* group had asymmetrically reduced thickness of left inferior frontal, temporal and parietal cortices, whereas the *C9ORF72* group had reduced thickness of right dorsal frontal, temporal and parietal cortices (Fig. 8).

In the diffusion tensor imaging analysis (Fig. 7), relative to healthy controls, the cases with *C9ORF72* mutation showed increased radial diffusivity and decreased fractional anisotropy bilaterally in anterior thalamic radiations, uncinate fasciculus, anterior cingulum and anterior corpus callosum; and in right posterior corpus callosum, posterior inferior longitudinal fasciculus and superior longitudinal fasciculus (all family-wise error corrected $P < 0.05$). In addition, the *C9ORF72* cases showed increased

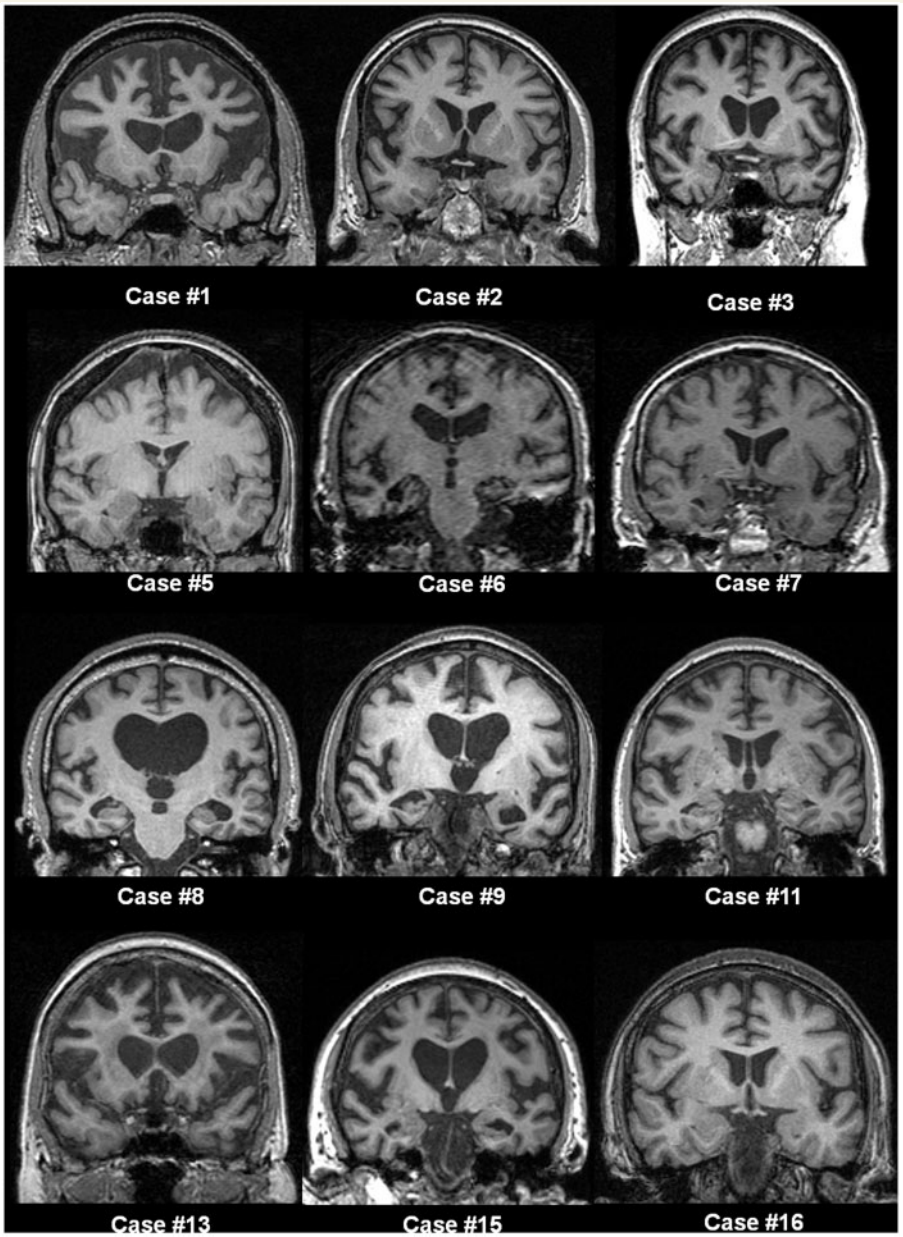

Figure 5 Representative T_1-weighted coronal magnetic resonance brain images for cases with *C9ORF72* mutation. Numbering of cases is as per Table 2. Patterns of atrophy were highly variable across the group, and no clear consistent profile of atrophy was evident visually. The distribution of atrophy was not prominently asymmetric between the cerebral hemispheres in most cases. Several cases had predominantly frontal lobe atrophy (Cases 1, 2 and 13), while temporal lobe atrophy was prominent in other cases (Cases 6 and 9). Other cases showed more generalized involvement with more prominent central atrophy (Cases 8 and 15) or minimal cross-sectional atrophy to visual inspection (Case 16).

radial diffusivity in left frontal superior longitudinal fasciculus and posterior corpus callosum, and in the right corticospinal tract.

Histopathological features

Genetic studies of the neuropathological FTLD cohort identified six cases with the *C9ORF72* repeat expansion. These cases were assessed in relation to a group of 53 'control' cases with FTLD-TDP [four cases with type B TDP-43 pathology (Mackenzie *et al.*, 2011), 11 type A cases with a *GRN* mutation, 17 type A cases without a *GRN* mutation and 21 type C cases]. TDP-43 pathology was evident in the hippocampus in all cases with FTLD-TDP irrespective of the presence of the *C9ORF72* repeat expansion. Four of the six cases with *C9ORF72* mutation were previously classified as FTLD-TDP type A while two cases had type B pathology. All six cases contained sparse to moderate numbers of compact and/or 'star-shaped' neuronal cytoplasmic inclusions in the granule cell layer of the hippocampal dentate gyrus. Sparse TDP-43-positive neuronal cytoplasmic inclusions were also found in the CA4 to CA1 hippocampal subregions with two cases also containing an

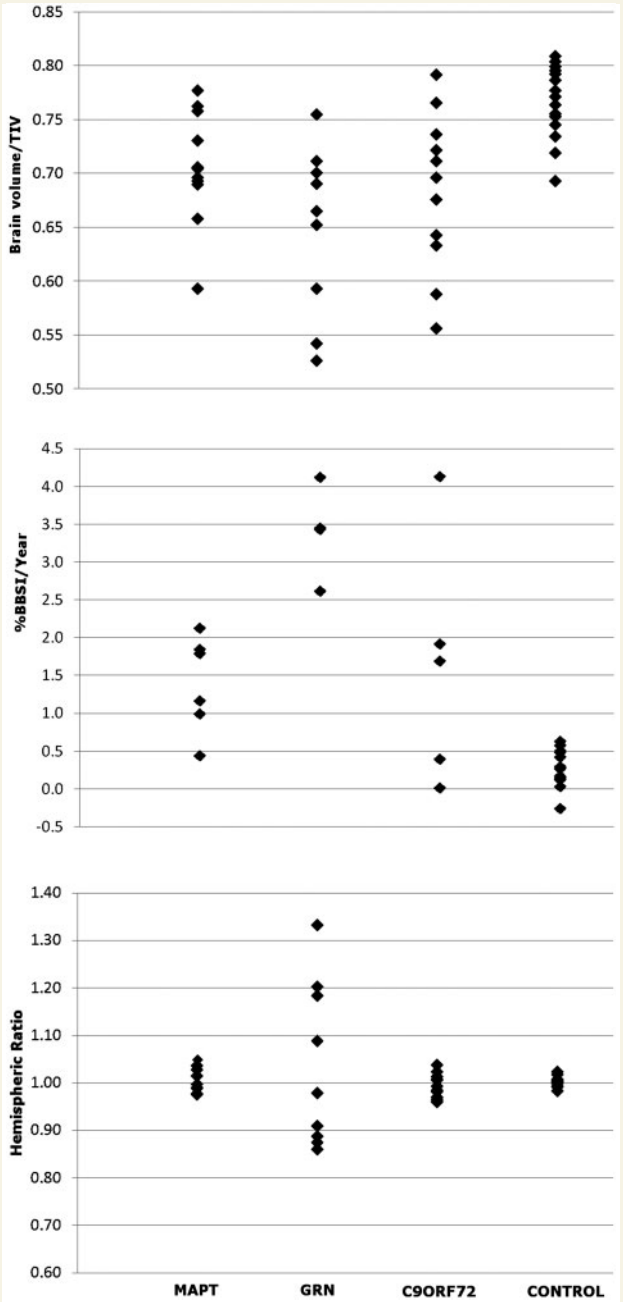

Figure 6 Individual brain volumes corrected for total intracranial volume (TIV) by group (*top*). Annualized percentage change in brain boundary shift integral (BBSI) by group (*middle*). Hemispheric asymmetry expressed as the ratio of left/right hemisphere volumes by subject and group (*bottom*).

occasional neuronal intranuclear inclusion. Variable numbers of TDP-43-positive neurites were also seen. No TDP-43 pathology was observed in the cerebellum of either the cases with *C9ORF72* mutation or FTLD-TDP controls.

All six cases with *C9ORF72* mutation contained p62-positive small, 'star-shaped' neuronal cytoplasmic inclusions in the granule cells of the hippocampal dentate gyrus. The numbers of such inclusions ranged from moderate to frequent where virtually all neurons contained neuronal cytoplasmic inclusions (Fig. 9) and similar p62-positive neuronal cytoplasmic inclusions were also found in variable numbers throughout the hippocampus from the CA4 to the CA1 subregions. P62 immunohistochemistry also highlighted neuritic structures. In all cases with *C9ORF72* mutation, p62-positive inclusions were strikingly more frequent than TDP-43-positive inclusions (Fig. 9A and B). In the control FTLD-TDP cases, the number of the p62-positive neuronal cytoplasmic inclusions in the hippocampal neurons including the granule cells of the dentate gyrus mirrored the frequency of TDP-43 immunoreactive neuronal cytoplasmic inclusions.

Small, p62-positive, but TDP-43-negative neuronal cytoplasmic inclusions were found in the cytoplasm of the cerebellar granule cells in all cases with *C9ORF72* mutation, but not in the control cases. The severity of the cerebellar pathology ranged from rare p62-positive neuronal cytoplasmic inclusions to severe involvement when nearly all granule cells appeared to contain an inclusion. It is of note that cases with high numbers of the p62-positive hippocampal inclusions also tended to have frequent p62-positive inclusions in the cerebellar granule cells.

Discussion

Here we present a detailed clinical, neuroanatomical and neuropathological analysis of a series of 19 cases with FTLD and the *C9ORF72* hexanucleotide repeat expansion representing 18 families in the UK. We confirm initial reports (Dejesus-Hernandez *et al.*, 2011; Gijselinck *et al.*, 2011; Renton *et al.*, 2011) that this mutation is an important cause of FTLD and FTLD–MND overlap syndromes, representing ~7% of our entire FTLD series, 8% of FTLD not otherwise accounted for by previously identified mutations, 35% of mutation-associated FTLD, 36% of FTLD with clinical evidence of MND and 4% of apparently sporadic FTLD. Identification of the *C9ORF72* mutation has allowed attribution of a specific genetic cause in 88% of all cases of autosomal dominant FTLD in this series. However, some 33% of *C9ORF72* mutation cases in this series had no known family history of FTLD or MND. In line with previous evidence in chromosome 9-linked FTLD and FTD–MND, age at onset (43–68 years), clinical duration (1.6 to >22 years) and clinical features were highly variable between and within families. The most common presenting syndrome was behavioural variant FTD, though around half of cases had an alternative syndrome at presentation, and over the course of follow-up ~60% of cases manifested at least some clinical features of MND. This substantial clinical heterogeneity is in line with previous reports describing chromosome 9-linked FTLD (Momeni *et al.*, 2006; Morita *et al.*, 2006; Vance *et al.*, 2006; Valdmanis *et al.*, 2007; Luty *et al.*, 2008; Le Ber *et al.*, 2009; Gijselinck *et al.*, 2010; Boxer *et al.*, 2011; Pearson *et al.*, 2011), and was reflected in a range of profiles of atrophy distribution and severity on neuroimaging of individual patients here. However, group-wise analyses comparing the *C9ORF72* mutation cases with healthy controls and with other mutation groups suggested certain common features that may constitute a core phenotype of this mutation.

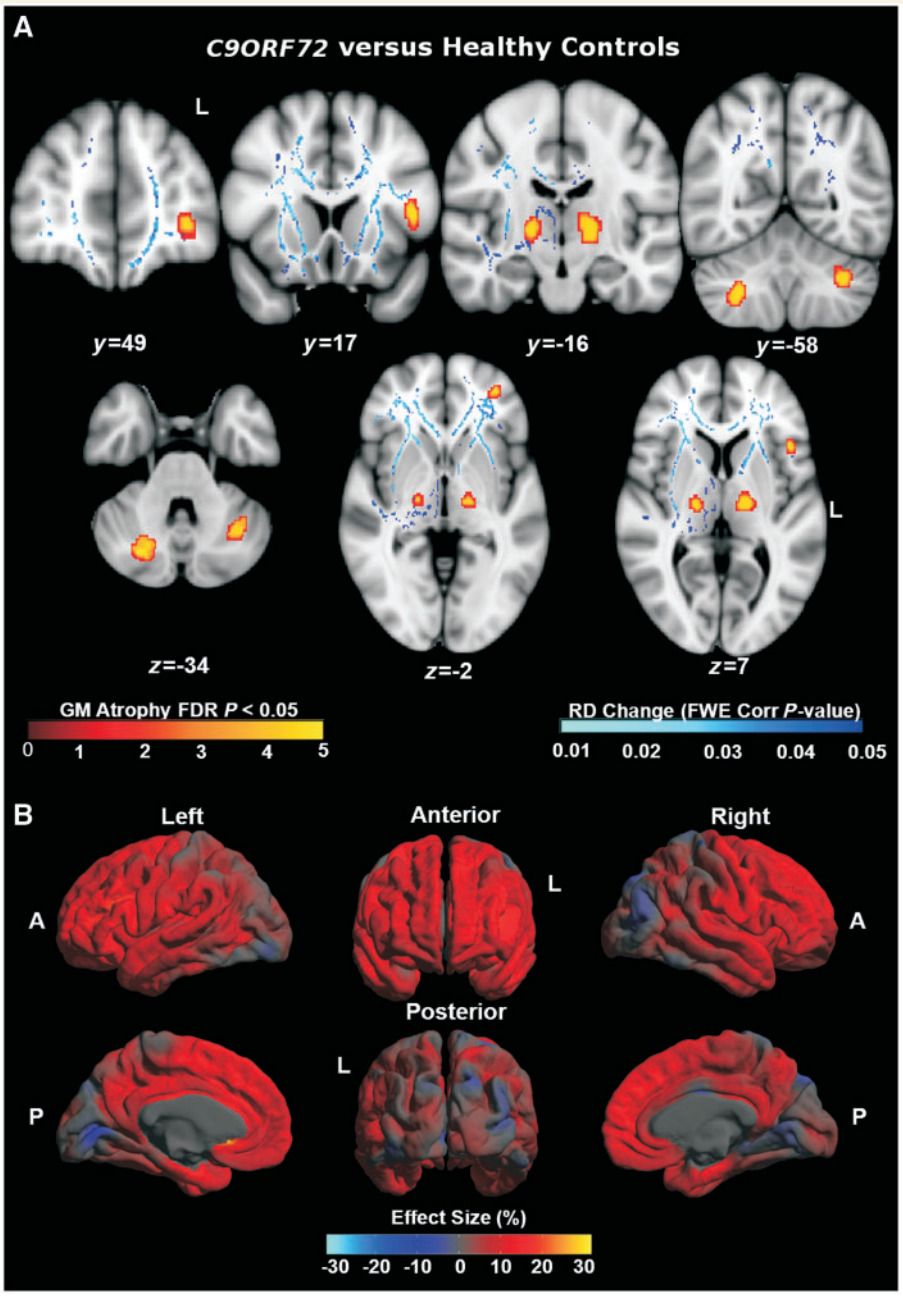

Figure 7 (**A**) Profiles of grey matter (GM) atrophy ($n = 11$) and increased radial diffusivity (RD) maps ($n = 3$) in *C9ORF72* cases versus healthy controls. MNI co-ordinates are displayed. (**B**) Mean difference in cortical thickness expressed as a percentage of the mean thickness in *C9ORF72* cases ($n = 11$) versus controls. A = anterior; FDR = false discovery rate; FWE = family-wise error; L = left; P = posterior.

Clinically, anxiety and agitated behaviour were early and prominent in a substantial proportion of our *C9ORF72* mutation cohort. These features were of sufficient significance here to lead to early contact with psychiatric services in several cases and a presumptive diagnosis of encephalitis in one case; it is possible that similar but less severe symptoms were exhibited by other cases but were de-emphasized in the context of other behavioural and cognitive deficits (a limitation of retrospective analyses). Neuropsychologically, alongside executive dysfunction, deficits of episodic memory were salient. Indeed, memory impairment dominated the clinical presentation in several cases, leading to an initial clinical diagnosis of Alzheimer's disease in two patients. Several previous detailed phenomenological and neuropsychological studies of FTLD have included patients presenting with prominent neuropsychiatric features (Omar *et al.*, 2009; Lillo *et al.*, 2010; Loy *et al.*, 2010) or episodic memory impairment (Hornberger *et al.*, 2010), raising the possibility that apparently sporadic cases of behavioural variant FTD sharing such phenotypic features may carry the *C9ORF72* repeat expansion. Dominant parietal lobe deficits (acalculia, apraxia) were frequent in the present

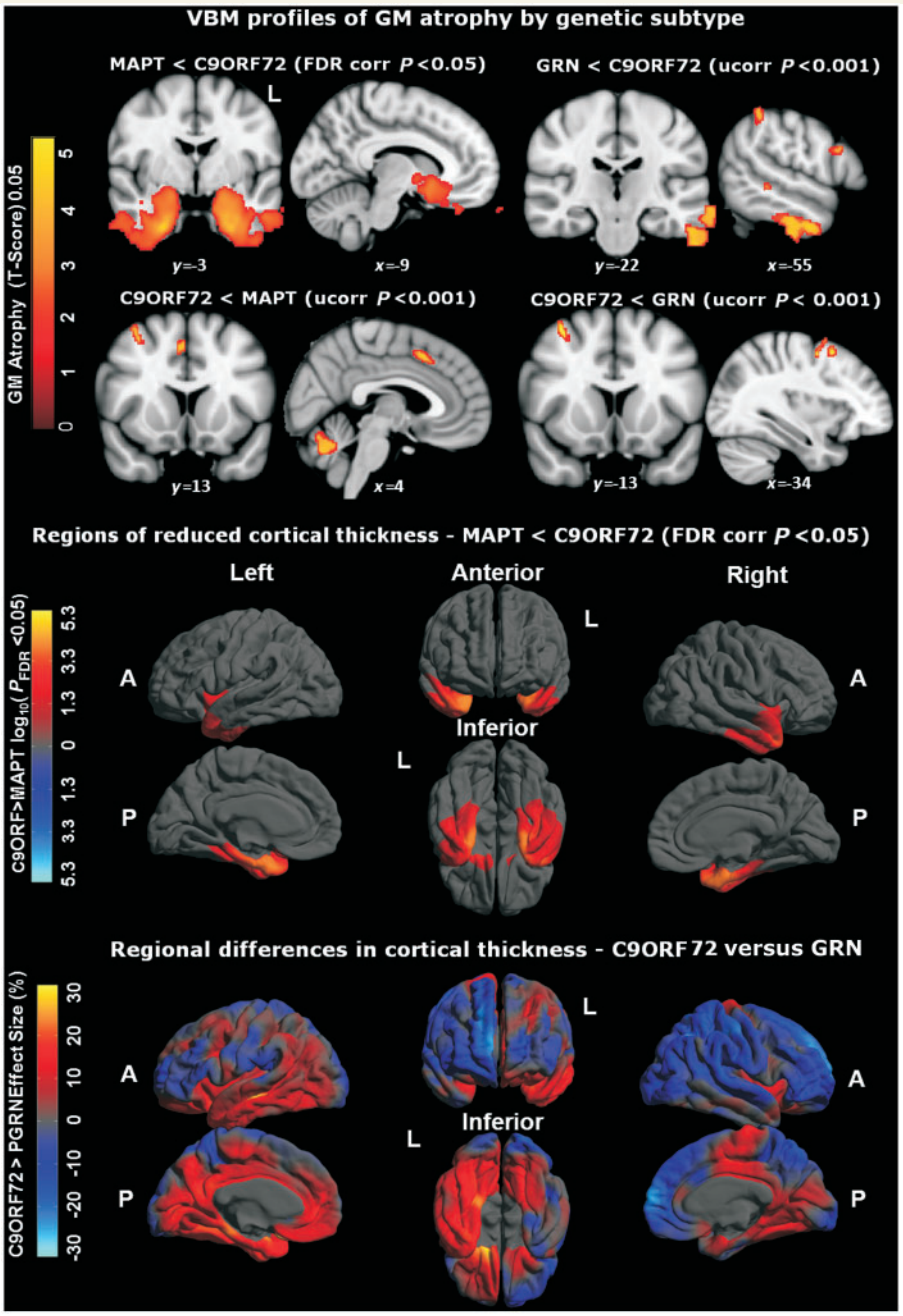

Figure 8 *Top*: Voxel-based morphometry (VBM) profiles of grey matter (GM) atrophy by genetic subtype; $P < 0.001$. MNI co-ordinates are displayed. *Middle:* regional reduction of cortical thickness in *MAPT* mutation carriers compared with *C9ORF72* mutation carriers. Colour scale for statistical difference represents FDR-corrected $P < 0.05$. *Bottom:* regional variation of cortical thickness in *GRN* mutation carriers compared with *C9ORF72* mutation carriers. Colour bar for per cent difference represents magnitude of cortical thickness group difference expressed as a percentage of the mean group thickness. Red and yellow (positive values) represent lower cortical thickness in the *GRN* group, whereas dark to light blue (negative values) represent lower cortical thickness in the *C9ORF72* group. A = anterior; FDR = false discovery rate; L = left; P = posterior; Ucorr = uncorrected.

C9ORF72 mutation cohort; it is of interest that clinical parietal lobe involvement was previously also found to be a common feature of *GRN* mutations (Rohrer *et al.*, 2008). Previous clinical series of chromosome 9-associated FTLD and FTD–MND have reported similar findings, with initial neuropsychiatric contact in a number of cases and clinical diagnoses including Alzheimer's disease and corticobasal degeneration (Morita *et al.*, 2006; Luty *et al.*, 2008; Lillo *et al.*, 2010; Boxer *et al.*, 2011; Murray *et al.*, 2011; Pearson *et al.*, 2011).

The group-wise neuroanatomical analyses here suggest candidate brain substrates for these clinical features. The *C9ORF72* mutation group showed extensive cortical loss involving frontal,

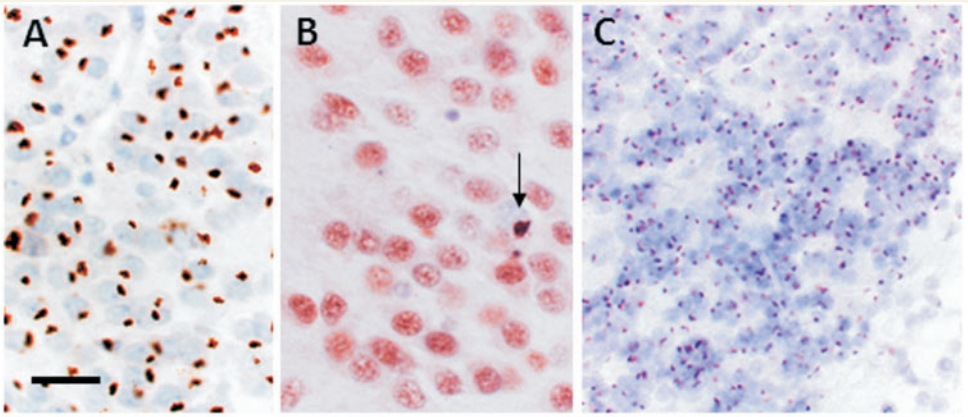

Figure 9 P62 and TDP-43 immunohistochemistry in FTLD-TDP with the *C9ORF72* hexanucleotide repeat expansion. Frequent p62-positive (**A**) and sparse TDP-43-positive (**B**, arrow) neuronal cytoplasmic inclusions were present in the granule cells of the dentate gyrus in a case with the *C9ORF72* repeat expansion. Numerous p62-positive neuronal cytoplasmic inclusions were also present in the cerebellar granule cell (**C**), which were negative for TDP-43. Scale bars: **A** = 50 μm; **B** = 30 μm; **C** = 80 μm.

temporal and parietal lobes that was relatively symmetric between cerebral hemispheres; while the voxel-based morphometry analysis showed grey matter loss in thalamus and cerebellum, and tractography demonstrated associated damage involving long subcortical projection pathways in the superior and inferior longitudinal fasciculi, cingulum, thalamic radiations and descending corticospinal tract, as well as the corpus callosum. The atrophy profile of *C9ORF72* mutation cases contrasts both with the relatively localized temporal lobe involvement associated with *MAPT* mutation cases and the strongly asymmetric profile in *GRN* cases. We speculate that the relatively sparse cortical correlates shown in the voxel-based morphometry analysis of the *C9ORF72* mutation cohort here may reflect wide inter-subject variation in cortical loss, with the more consistent involvement of subcortical grey matter structures (including thalamus and cerebellum) being a more robust signature of this mutation. We do not argue that the neuroanatomical signature of the *C9ORF72* repeat expansion is restricted to these regions; subcortical structures typically act as hubs within structural and functional networks (Van der Werf *et al.*, 2003; Schmahmann and Pandya, 2008; Tedesco *et al.*, 2011), with projection targets that include other sites of pathological involvement (for example, the thalamus participates in a diencephalic network that also includes the hippocampi). The diffuse projections of these subcortical structures may account for the wide range of cognitive findings and cortical damage exhibited across the *C9ORF72* mutation cohort here. Involvement of thalamus and cerebellar connections could underpin the prominent neuropsychiatric features shown by these cases (Andreasen *et al.*, 1996; Schmahmann, 2005; Goossens *et al.*, 2007; Straube *et al.*, 2007; Schmahmann and Pandya, 2008; Tedesco *et al.*, 2011), as well as episodic memory deficits (Van der Werf *et al.*, 2003; de Jong *et al.*, 2008) somatic complaints, hallucinations and delusions (Kessler *et al.*, 2009; Tedesco *et al.*, 2011). Although none of our cases had frank cerebellar ataxia, this has been described in previous cases of chromosome 9 linked FTLD (Pearson *et al.*, 2011).

Neuropathological assessment of six cases with the *C9ORF72* repeat expansion demonstrated a heterogeneous profile, in that both FTLD-TDP type A and type B morphological patterns were represented. Similar histomorphological heterogeneity has been emphasized in previous neuropathological analyses of *C9ORF72* mutation cases (Murray *et al.*, 2011). In addition, all our *C9ORF72* mutation cases had p62-positive neuronal cytoplasmic inclusions prominently in excess of TDP-43-positive neuronal cytoplasmic inclusions in the granule cells of the hippocampal dentate gyrus and other hippocampal subregions as well as p62-positive, TDP-43-negative inclusions in cerebellar granule cells. Our findings are supported by a recent publication that proposes this pattern of proteinopathy as pathognomonic for the *C9ORF72* hexanucleatide repeat insertion (Al-Sarraj *et al.*, 2011). The ubiquitin-binding protein 62 (p62) or sequestosome 1 (like ubiquitin itself) is a common component of neuronal and glial proteinaceous inclusions in a range of neurodegenerative diseases including FTLD-TDP. It has been previously shown in a proportion of cases with FTLD-TDP that p62 (and, to a lesser extent, ubiquitin) immunohistochemistry may highlight a larger number of neuronal cytoplasmic inclusions in the dentate granule cells than are demonstrated on TDP-43 immunohistochemistry and that small dot-like or star-shaped p62-positve, TDP-43-negative inclusions may be present in the granule cells of the cerebellar cortex (Pikkarainen *et al.*, 2008; King *et al.*, 2011). Furthermore, ubiquitin-positive neuronal cytoplasmic inclusions in cerebellar granule cells have also been documented in FTD–MND linked to chromosome 9 due to the *C9ORF72* repeat expansion (Dejesus-Hernandez *et al.*, 2011). The present neuropathological data support the notion that 'excess' p62 pathology may be a characteristic feature of the *C9ORF72* repeat expansion. It is noteworthy that the sites of heavy p62 involvement identified here, including hippocampi and cerebellum, are likely to be pathophysiologically relevant based on clinical and neuroimaging findings in the present cohort. Moreover, these findings corroborate previous neuropathological evidence in other cohorts. However, the origin and

true significance of the excess p62 labelling identified here require further investigation, including quantitative analysis of p62 deposition within and between brain regions. In addition, the present series comprised exclusively cases presenting with FTLD; there may be a stratification of histopathological findings across the broader phenotypic spectrum of the *C9ORF72* mutations, which also includes cases presenting with MND (Al-Sarraj *et al.*, 2011; Murray *et al.*, 2011).

In summary, our findings suggest that clinicians should consider the *C9ORF72* repeat expansion in patients with FTLD, particularly with clinical evidence (or a family history) of MND or with prominent anxiety or memory impairment. From a neurobiological perspective, our data suggest that involvement of a subcortical network may underpin the wide-ranging phenotypic features of the *C9ORF72* repeat expansion. Recent clinico-anatomico-pathological evidence in FTLD suggests that phenotypes arise from an interaction of molecular and network-specific factors (Schmahmann and Pandya, 2008; Rohrer *et al.*, 2011). This hypothesis could be tested specifically in *C9ORF72* mutation cases by targeting potentially relevant cognitive operations and network anatomy (Tedesco *et al.*, 2011). Neuropathologically, excess p62 deposition within the culprit network may be a signature of the *C9ORF72* mutation. Future work should analyse these cases prospectively and in relation to other mutation groups, with joint longitudinal behavioural and neuroimaging (including connectivity-based) methods, and detailed genotypic stratification and histopathological correlation.

Acknowledgements

We thank all subjects and their families for their participation.

Funding

This work was undertaken at UCLH/UCL who received a proportion of funding from the Department of Health's NIHR Biomedical Research Centres funding scheme. The Dementia Research Centre is an Alzheimer's Research UK Co-ordinating Centre. This work was also funded by the Medical Research Council UK and by the Wellcome Trust. C.J.M. is supported by an MRC programme grant. N.C.F. is a NIHR senior investigator and MRC Senior Clinical Fellow. J.D.W. is supported by a Wellcome Trust Senior Clinical Fellowship (091673/Z/10/Z).

References

Al-Sarraj S, King A, Troakes C, Smith B, Maekawa S, Bodi I, et al. p62 positive, TDP-43 negative, neuronal cytoplasmic and intranuclear inclusions in the cerebellum and hippocampus define the pathology of C9orf72-linked FTLD and MND/ALS [Internet]. Acta Neuropathologica 2011. Available from: http://www.springerlink.com/index/10.1007/s00401-011-0911-2 (23 November 2011, date last accessed).

Andreasen NC, O'Leary DS, Cizadlo T, Arndt S, Rezai K, Ponto LL, et al. Schizophrenia and cognitive dysmetria: a positron-emission tomography study of dysfunctional prefrontal-thalamic-cerebellar circuitry. Proc Natl Acad Sci USA 1996; 93: 9985–90.

Beck J, King A, Scahill R, Warren JD, Fox NC, Rossor MN, et al. A distinct clinical, neuropsychological and radiological phenotype is associated with progranulin gene mutations in a large UK series. Brain 2008; 131: 706–20.

Boeve BF, Lang AE, Litvan I. Corticobasal degeneration and its relationship to progressive supranuclear palsy and frontotemporal dementia. Ann Neurol 2003; 54 (Suppl 5): S15–S19.

Boxer AL, Mackenzie IR, Boeve BF, Baker M, Seeley WW, Crook R, et al. Clinical, neuroimaging and neuropathological features of a new chromosome 9p-linked FTD-ALS family. J Neurol Neurosurg Psychiatr 2011; 82: 196–203.

Cook P, Bai Y, Nedjati-Gilani S, Seunarine K, Hall M, Parker G, et al. Camino: open-source diffusion-MRI reconstruction and processing. Seattle, WA, USA: International Society for Magnetic Resonance in Medicine; 2006. p. 2759.

Dale AM, Fischl B, Sereno MI. Cortical surface-based analysis. I. Segmentation and surface reconstruction. Neuroimage 1999; 9: 179–94.

de Jong LW, van der Hiele K, Veer IM, Houwing JJ, Westendorp RGJ, Bollen ELEM, et al. Strongly reduced volumes of putamen and thalamus in Alzheimer's disease: an MRI study. Brain 2008; 131: 3277–85.

Dejesus-Hernandez M, Mackenzie IR, Boeve BF, Boxer AL, Baker M, Rutherford NJ, et al. Expanded GGGGCC hexanucleotide repeat in noncoding region of C9ORF72 causes chromosome 9p-linked FTD and ALS [Internet]. Neuron 2011. Available from: http://www.ncbi.nlm.nih.gov/pubmed/21944778 (19 October 2011, date last accessed).

Fischl B, Dale AM. Measuring the thickness of the human cerebral cortex from magnetic resonance images. Proc Natl Acad Sci USA 2000; 97: 11050–5.

Fletcher PD, Warren JD. Semantic Dementia: a specific network-opathy [Internet]. J Mol Neurosci 2011. Available from: http://www.ncbi.nlm.nih.gov/pubmed/21710360 (17 August 2011, date last accessed).

Freeborough PA, Fox NC. The boundary shift integral: an accurate and robust measure of cerebral volume changes from registered repeat MRI. IEEE Trans Med Imaging 1997; 16: 623–9.

Freeborough PA, Fox NC, Kitney RI. Interactive algorithms for the segmentation and quantitation of 3-D MRI brain scans. Comput Methods Programs Biomed 1997; 53: 15–25.

Gijselinck I, Engelborghs S, Maes G, Cuijt I, Peeters K, Mattheijssens M, et al. Identification of 2 Loci at chromosomes 9 and 14 in a multiplex family with frontotemporal lobar degeneration and amyotrophic lateral sclerosis. Arch Neurol 2010; 67: 606–16.

Gijselinck I, Van Langenhove T, van der Zee J, Sleegers K, Philtjens S, Kleinberger G, et al. A C9orf72 promoter repeat expansion in a Flanders-Belgian cohort with disorders of the frontotemporal lobar degeneration-amyotrophic lateral sclerosis spectrum: a gene identification study. Lancet Neurol 2011. Dec 7 [Epub ahead of print].

Goldman JS, Farmer JM, Wood EM, Johnson JK, Boxer A, Neuhaus J, et al. Comparison of family histories in FTLD subtypes and related tauopathies. Neurology 2005; 65: 1817–9.

Goossens L, Schruers K, Peeters R, Griez E, Sunaert S. Visual presentation of phobic stimuli: amygdala activation via an extrageniculostriate pathway? Psychiatry Res 2007; 155: 113–20.

Gorno-Tempini ML, Hillis AE, Weintraub S, Kertesz A, Mendez M, Cappa SF, et al. Classification of primary progressive aphasia and its variants. Neurology 2011; 76: 1006–14.

Hornberger M, Piguet O, Graham AJ, Nestor PJ, Hodges JR. How preserved is episodic memory in behavioral variant frontotemporal dementia? Neurology 2010; 74: 472–9.

Kessler RM, Woodward ND, Riccardi P, Li R, Ansari MS, Anderson S, et al. Dopamine D2 receptor levels in striatum, thalamus, substantia nigra, limbic regions, and cortex in schizophrenic subjects. Biol Psychiatr 2009; 65: 1024–31.

King A, Maekawa S, Bodi I, Troakes C, Al-Sarraj S. Ubiquitinated, p62 immunopositive cerebellar cortical neuronal inclusions are evident across the spectrum of TDP-43 proteinopathies but are only rarely

additionally immunopositive for phosphorylation-dependent TDP-43. Neuropathology 2011; 31: 239–49.

Lashley T, Rohrer JD, Bandopadhyay R, Fry C, Ahmed Z, Isaacs AM, et al. A comparative clinical, pathological, biochemical and genetic study of fused in sarcoma proteinopathies. Brain 2011; 134: 2548–64.

Le Ber I, Camuzat A, Berger E, Hannequin D, Laquerrière A, Golfier V, et al. Chromosome 9p-linked families with frontotemporal dementia associated with motor neuron disease. Neurology 2009; 72: 1669–76.

Le Ber I, Camuzat A, Hannequin D, Pasquier F, Guedj E, Rovelet-Lecrux A, et al. Phenotype variability in progranulin mutation carriers: a clinical, neuropsychological, imaging and genetic study. Brain 2008; 131: 732–46.

Lillo P, Garcin B, Hornberger M, Bak TH, Hodges JR. Neurobehavioral features in frontotemporal dementia with amyotrophic lateral sclerosis. Arch Neurol 2010; 67: 826–30.

Litvan I, Agid Y, Calne D, Campbell G, Dubois B, Duvoisin RC, et al. Clinical research criteria for the diagnosis of progressive supranuclear palsy (Steele-Richardson-Olszewski syndrome): report of the NINDS-SPSP international workshop. Neurology 1996; 47: 1–9.

Loy CT, Kril JJ, Trollor JN, Kiernan MC, Kwok JB, Vucic S, et al. The case of a 48 year-old woman with bizarre and complex delusions. Nat Rev Neurol 2010; 6: 175–9.

Luty AA, Kwok JBJ, Thompson EM, Blumbergs P, Brooks WS, Loy CT, et al. Pedigree with frontotemporal lobar degeneration–motor neuron disease and Tar DNA binding protein-43 positive neuropathology: genetic linkage to chromosome 9. BMC Neurol 2008; 8: 32.

Mackenzie IRA, Neumann M, Baborie A, Sampathu DM, Plessis D, Jaros E, et al. A harmonized classification system for FTLD-TDP pathology. Acta Neuropathologica 2011; 122: 111–3.

Momeni P, Schymick J, Jain S, Cookson MR, Cairns NJ, Greggio E, et al. Analysis of IFT74 as a candidate gene for chromosome 9p-linked ALS-FTD. BMC Neurol 2006; 6: 44.

Morita M, Al-Chalabi A, Andersen PM, Hosler B, Sapp P, Englund E, et al. A locus on chromosome 9p confers susceptibility to ALS and frontotemporal dementia. Neurology 2006; 66: 839–44.

Murray ME, Dejesus-Hernandez M, Rutherford NJ, Baker M, Duara R, Graff-Radford NR, et al. Clinical and neuropathologic heterogeneity of c9FTD/ALS associated with hexanucleotide repeat expansion in C9ORF72 [Internet]. Acta Neuropathologica 2011. Available from: http://www.ncbi.nlm.nih.gov/pubmed/22083254 (21 November 2011, date last accessed).

Omar R, Sampson EL, Loy CT, Mummery CJ, Fox NC, Rossor MN, et al. Delusions in frontotemporal lobar degeneration. J Neurol 2009; 256: 600–7.

Pearson JP, Williams NM, Majounie E, Waite A, Stott J, Newsway V, et al. Familial frontotemporal dementia with amyotrophic lateral sclerosis and a shared haplotype on chromosome 9p. J Neurol 2011; 258: 647–55.

Pikkarainen M, Hartikainen P, Alafuzoff I. Neuropathologic features of frontotemporal lobar degeneration with ubiquitin-positive inclusions visualized with ubiquitin-binding protein p62 immunohistochemistry. J Neuropathol Exp Neurol 2008; 67: 280–98.

Rademakers R, Baker M, Gass J, Adamson J, Huey ED, Momeni P, et al. Phenotypic variability associated with progranulin haploinsufficiency in patients with the common 1477C–>T (Arg493X) mutation: an international initiative. Lancet Neurol 2007; 6: 857–68.

Rascovsky K, Hodges JR, Knopman D, Mendez MF, Kramer JH, Neuhaus J, et al. Sensitivity of revised diagnostic criteria for the behavioural variant of frontotemporal dementia. Brain 2011; 134: 2456–77.

Ratnavalli E, Brayne C, Dawson K, Hodges JR. The prevalence of frontotemporal dementia. Neurology 2002; 58: 1615–21.

Renton AE, Majounie E, Waite A, Simón-Sánchez J, Rollinson S, Gibbs JR, et al. A hexanucleotide repeat expansion in C9ORF72 is the cause of chromosome 9p21-linked ALS-FTD [Internet]. Neuron 2011. Available from: http://www.ncbi.nlm.nih.gov/pubmed/21944779 (19 October 2011, date last accessed).

Ridgway GR, Omar R, Ourselin S, Hill DLG, Warren JD, Fox NC. Issues with threshold masking in voxel-based morphometry of atrophied brains. Neuroimage 2009; 44: 99–111.

Rohrer JD, Guerreiro R, Vandrovcova J, Uphill J, Reiman D, Beck J, et al. The heritability and genetics of frontotemporal lobar degeneration. Neurology 2009; 73: 1451–6.

Rohrer J, Lashley T, Schott J. Clinical and neuroanatomical signatures of tissue pathology in fontotemporal lobar degeneration. Brain 2011; 134: 2565–81.

Rohrer JD, Ridgway GR, Modat M, Ourselin S, Mead S, Fox NC, et al. Distinct profiles of brain atrophy in frontotemporal lobar degeneration caused by progranulin and tau mutations. Neuroimage 2010; 53: 1070–6.

Rohrer JD, Warren JD. Phenotypic signatures of genetic frontotemporal dementia [Internet]. Curr Opin Neurol 2011. Available from: http://www.ncbi.nlm.nih.gov/pubmed/21986680 (9 November 2011, date last accessed).

Rohrer JD, Warren JD, Omar R, Mead S, Beck J, Revesz T, et al. Parietal lobe deficits in frontotemporal lobar degeneration caused by a mutation in the progranulin gene. Arch Neurol 2008; 65: 506–13.

Schmahmann JD. Cognition, emotion and the cerebellum. Brain 2005; 129: 290–2.

Schmahmann J, Pandya D. Disconnection syndromes of basal ganglia, thalamus, and cerebrocerebellar systems. Cortex 2008; 44: 1037–66.

Seelaar H, Rohrer JD, Pijnenburg YAL, Fox NC, van Swieten JC. Clinical, genetic and pathological heterogeneity of frontotemporal dementia: a review. J Neurol Neurosurg Psychiatr 2011; 82: 476–86.

Smith SM, Jenkinson M, Johansen-Berg H, Rueckert D, Nichols TE, Mackay CE, et al. Tract-based spatial statistics: voxelwise analysis of multi-subject diffusion data. Neuroimage 2006; 31: 1487–505.

Smith SM, Nichols TE. Threshold-free cluster enhancement: addressing problems of smoothing, threshold dependence and localisation in cluster inference. Neuroimage 2009; 44: 83–98.

Straube T, Mentzel H-J, Miltner WHR. Waiting for spiders: brain activation during anticipatory anxiety in spider phobics. Neuroimage 2007; 37: 1427–36.

Tedesco AM, Chiricozzi FR, Clausi S, Lupo M, Molinari M, Leggio MG. The cerebellar cognitive profile [Internet]. Brain 2011. Available from: http://www.ncbi.nlm.nih.gov/pubmed/22036960 (9 November 2011, date last accessed).

Valdmanis PN, Dupre N, Bouchard J-P, Camu W, Salachas F, Meininger V, et al. Three families with amyotrophic lateral sclerosis and frontotemporal dementia with evidence of linkage to chromosome 9p. Arch Neurol 2007; 64: 240–5.

Van der Werf YD, Scheltens P, Lindeboom J, Witter MP, Uylings HBM, Jolles J. Deficits of memory, executive functioning and attention following infarction in the thalamus; a study of 22 cases with localised lesions. Neuropsychologia 2003; 41: 1330–44.

Vance C, Al-Chalabi A, Ruddy D, Smith BN, Hu X, Sreedharan J, et al. Familial amyotrophic lateral sclerosis with frontotemporal dementia is linked to a locus on chromosome 9p13.2-21.3. Brain 2006; 129: 868–76.